Lab on a Chip

Cite this: *Lab Chip*, 2012, **12**, 3624–3636

www.rsc.org/loc

CRITICAL REVIEW

Optically-actuated translational and rotational motion at the microscale for microfluidic manipulation and characterization†

Samarendra Mohanty*

Received 10th May 2012, Accepted 16th July 2012
DOI: 10.1039/c2lc40538e

The single beam optical trap (optical tweezers), a highly focused beam, is on its way to revolutionizing not only the fields of colloidal physics and biology, but also materials science and engineering. Recently, spatially-extended three-dimensional light patterns have gained considerable usage for exerting force to alter, manipulate, organize and characterize materials. To advance the degree of manipulation, such as rotation of materials in microfluidic environments along with spatial structuring, other beam parameters such as phase and polarization have to be configured. These advances in optical tweezers' technology have enabled complex microfluidic actuation and sorting. In addition to remotely (in a non-contact way) applying force and torques in three-dimensions, which can be continuously varied unlike mechanical manipulators, optical tweezers-based methods can be used for sensing the force of interaction between microscopic objects in a microfluidic environment and for the characterization of micro-rheological properties. In this review, we place emphasis on applications of optical actuation based on novel beams in performing special functions such as rotation, transportation, sorting and characterization of the microscopic objects. Further, we have an extended discussion on optical actuation (transport and rotation) with fiber optic microbeams and spectroscopic characterization in the microfluidic environment. All these advancements in optical manipulation would further facilitate the growing use of optical tools for complex microfluidic manipulations.

Biophysics and Physiology Lab, Department of Physics, University of Texas-Arlington, TX 76019 E-mail: smohanty@uta.edu
† Published as part of a themed issue on optofluidics.

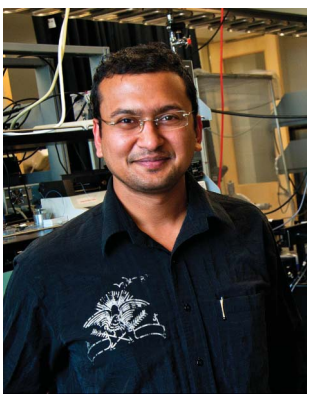

Samarendra Mohanty

Prof. Samar Mohanty leads the Biophysics and Physiology Group at University of Texas, Arlington. Samar did his postdoctoral training at the Beckman Laser Institute and Medical Clinic. He has worked as a scientist in the Center for Advanced Technology and has carried out biophotonics research in India, Germany, Italy, UK and Singapore. He uses photonics technology (optical tweezers, laser scissors, multiphoton/confocal microscopy, near-field scanning optical microscopy, digital holographic microscopy) combined with nanotechnology, microfluidics, genetics, and electrical tools for manipulating and imaging molecular and cellular processes from single molecule to the whole organism level. He has over 80 research papers and several patents.

A. Introduction and principle of optical manipulation

At the microscale, the force exerted by light is significant enough to levitate,[1–3] transport,[4] and even immobilize[5–7] objects. While laser beams with Gaussian intensity profiles have been widely used for optical micro-manipulation, novel beams (Laguerre–Gaussian,[8] Bessel[9] and Airy[10]) are now also utilized for specialized functions. Optical manipulation of large objects can be realized due to the fact that refraction (bending) of light leads to transfer of recoil-momentum to the object in order to trap it.[5] Optical trapping of nanoscale objects can be attributed to the induced electric dipole moment in the object which leads to a gradient force towards the highest intensity point in the focus.[11]

Single beam optical trapping or optical tweezers[5–7] (Fig. 1) provides a unique way of manoeuvring microscale objects without requiring direct contact with the object. Further, novel beams have enabled rotation[12] and even separation[13] of microscopic objects. The radiation pressure from absorption and scattering acts in opposition to the axial gradient force and therefore stable single-beam trapping requires high numerical aperture (NA) focusing optics such as microscope objectives,[14] or micro-optics[15] constructed on tip of an optical fiber. An unbeatable advantage of optical manipulation methods is the ability to work inside closed objects such as a living biological cell[14] or a microfluidic chip.[16] In recent years, spatial sculpting of

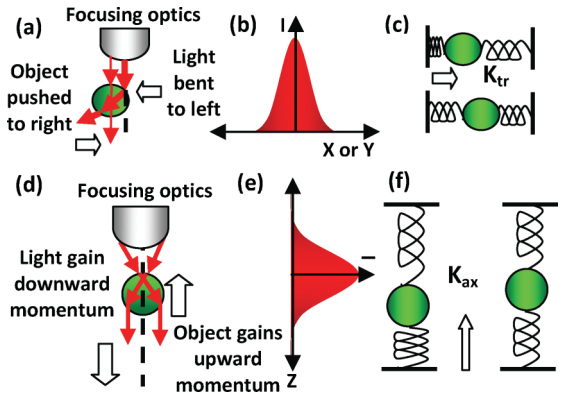

Fig. 1 Optical tweezers made up by a strongly focused laser beam to hold objects in three-dimensions. (a) Schematic ray-optics representation of the interaction between a laser beam and high-index object (in the Mie regime) giving rise to trapping in the transverse plane (XY) and the transverse intensity profile (b). A mechanical analogue of the object in the potential well displaced (ΔX) from center of the beam (c) and brought to the equilibrium position by spring-like action defined by constant K_{tr}. The nature of the transverse gradient force ($F_{tr} = -K_{tr}\Delta X$) for a high-index particle in a Gaussian beam is attractive to the highest intensity point. (d) Ray-optics representation of axial trapping (Z). In addition to wavelength, the spread of the intensity profile along the Z-direction (e) is dependent on the focal length of the focusing element and is defined by the Rayleigh range. (f) The classical mechanics representation of the axial displacement (ΔZ) and equilibrium position. The axial gradient trapping force ($F_{ax} = -K_{ax}\Delta Z$) towards the focus competes with the scattering force (away from the focus).

the potential landscape has been carried out using diffractive optical elements[17] for complex microfluidic manipulations. The spatially-extended optical tweezers have been deployed to hold hundreds of objects in three-dimensions in parallel,[17] which can then be fixed (*e.g.* by gelling). Micro-lens array based optical tweezers have also been integrated[18] with microfluidic platforms for trapping of cellular arrays and cytometric analysis.

Fig. 2a shows the schematic of holographic optical tweezers generated by a spatial light modulator (SLM), which has enabled assembly of a three-dimensional colloidal quasicrystal[19] (Fig. 2b). Multibeam optical traps have also been employed[20] for the assembly of microscale components (Fig. 2c).

It may be worth noting here that microscopic objects in a light-field can interact with each other by exchange of photons and thus can be coupled with each other by optical binding.[21–24] Though the optical binding force[21] falls away rapidly with distance, it cannot be neglected during nearest-neighbor interactions between objects under an optical field. Therefore, movement of one of the coupling partners can influence the position of the other and therefore organization of the whole assembly.[25] It is possible to deduce the patterning of particle assembly on the basis of pair interactions.[26,27] Besides construction of user-defined structures, optical tweezers are finding important applications in the characterization of materials including their microrheological[28,29] and other physico-chemical properties.[30] Finally, optical tweezers have turned out to be a valuable tool in studies of soft biological matter in microfluidic environments. Optical tweezers are ideally suited to manipulate cell membranes,[31] intra-cellular organelles and single molecules;[32,33] and also to characterize forces[34] between them.

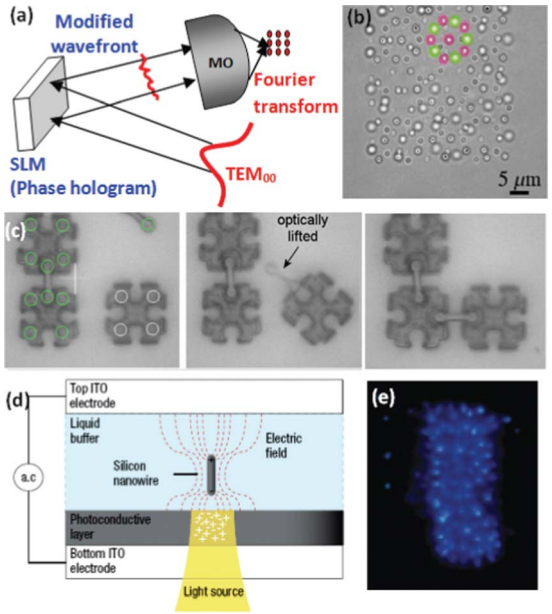

Fig. 2 Organization and assembly at the microscale. (a) Principle of holographic optical tweezers, (b) holographic assembly of a three-dimensional colloidal quasicrystal.[19] The shaded region identifies one embedded icosahedron. (c) Optical microassembly of photopolymerized components.[20] (d) Optoelectronic tweezers device structure and (e) collection of silver nanowires.[35]

Though several comprehensive literature reviews on optical tweezers-related technologies exist,[14,33,34] this review focuses on the construction, characterization and actuation of microscale objects for microfluidic applications, by conventional as well as fiber-optic trapping beams.

Optical tweezers[6] are gentle and act with forces that can be varied continuously in the femto- to hundreds of pico-Newton range by varying the power of the laser beam. By measuring the displacement of a probe particle from the center of the potential well of a calibrated trap in response to the presence of other objects or substrates, the force of interaction can be measured in real time with sub-fN resolution. The trapping stiffness (K_{tr}) can be determined either by the viscous drag, or by the equipartition or corner frequency measurements.[36] It may be noted that for bigger metallic and low- refractive index objects[37] such as aerosols, the gradient force is opposite to that of a high refractive index particle. In the Rayleigh regime, the tweezing effect can be explained as an electromagnetic field of the light inducing a dipole, thus pulling the object into the center of the beam where its energy is minimized.

Since the trapping force is proportional to polarizability (which varies as the cube of the particle radius) for nano-objects, optical trapping and manipulation becomes increasingly difficult as size decreases to the nano-scale. Though nano-objects have been manipulated using optical tweezers,[38] the high polarizability of metallic objects[11] provides a better avenue for use as handles or probes to manipulate other objects. Further, surface plasmon resonance (SPR) near metallic surfaces (or nanoparticles) has been theorized[39] to enhance the trapping of dielectric nanoparticles. However, this enhancement may be achieved experimentally only by avoiding heating due to the resonant

optical tweezers' beam.[40] New approaches are being proposed and implemented to enhance the trapping efficiency with which objects can be manipulated. For example, a recent theoretical study[41] showed that a laser tuned to resonate with the internal energy levels of semiconductor nanoparticles could strengthen the trapping force up to 100 000 times. This enhancement occurs because resonance exaggerates the particle's polarization, which causes it to scatter more photons. The advent of optoelectronic tweezers[35] (a hybrid method where optical intensity of several orders of magnitude lower than optical tweezers is applied to a localized area of a photoconductive surface to allow flow of electric field, Fig. 2d) could concentrate arrays of silver nanowire (Fig. 2e). Due to the very low light-intensity requirement, optoelectronic tweezers hold great promise for lab-on-a-chip micromanipulation applications. Further, wide area manipulation is possible through near-field trapping (realized by total internal reflection), without the requirement of tight focusing since the intensity gradient in the near-field is naturally very sharp owing to the evanescent nature of the wave.[42]

B. Optical manipulation in a microfluidic environment

(i) Optical transport of microscopic objects

The efficient transport of materials is paramount for nano and biotechnological applications in lab-on-a-chip devices. Transport of several subunits may be required for isolation, to construct a material, to initiate a reaction, or even for processing the assembled structures. The simplest method is to move the optical tweezers, holding the object(s), to the desired location at a speed such that the trapped object(s) does not escape the optical potential. Unlike other mechanical means of transport, optical tweezers-based transport can be realized in closed environments such as living cells,[14,43] and microfluidic chips[44] without necessitating fluid movement. This has significant advantages as demonstrated in a recent study, where the translational actuation of an optically-trapped microsphere-lens in front of the exit port of a waveguide led to deflection of the beam (originating from the waveguide) in a range of directions.[45]

The dynamic (or active) optical tweezers can be used for the isolation of fluorescently labeled cells by optically transporting them from the analysis region to the collection channel[44] (Fig. 3a). In contrast to the dynamic optical beams, passive optical transport can be realized over large distances along the laser beam using the scattering force from a Gaussian[46] or Bessel beam,[47] in particular due to its propagation-invariance nature. The central maximum of a Bessel beam (generated by axicon[48]) has a non-diffracting line focus in the axial direction and a transverse profile such that beam remains unaltered during propagation.

The scattering force based method is not applicable for transport in transverse directions, which may limit manipulation and visualization of the microscopic objects in a lab-on-a-chip device. To enable efficient transverse transport in a microfluidic environment, asymmetric line tweezers have been introduced.[49] The transversely asymmetric potential well was realized by tilting an astigmatic laser beam (generated by a cylindrical lens) with respect to the optical axis of the microscope objective so as to generate a coma along the major axis of the astigmatic intensity profile. Objects experience an asymmetric gradient force as well as a non-zero transverse component of the scattering force acting along the direction of flatter potential of the line tweezers and are passively transported.[52]

This spatially-sculpted method has been utilized to transport microscopic objects including cells,[49] intra-cellular objects,[53] nanotubes,[52] and other colloidal particles.[49] Fig. 3b shows time-lapse images of transportation of polystyrene microspheres (1.4 μm) inside a microfluidic channel using asymmetric line tweezers (unpublished results). It may be noted that multiple asymmetric potential landscapes can be generated by diffractive optical elements, which will provide an increased ability for the parallel transportation of microscopic objects to different microfluidic chambers in an efficient and passive manner.

Recently, transportation in three-dimensions was achieved[10] by use of optical tweezers based on an Airy beam profile (upper panel, Fig. 3c). In addition to the propagation-invariance nature (as exists in Bessel beam), Airy beams result in acceleration in the transverse direction. Therefore, for transverse transport of microscopic objects it provides significant advantages over a Bessel beam. Such a beam can be described by a parabolic envelope of rays and is healed after an (axial) distance (Z_h) even after obstructing the beam transversely (by s, as shown in Fig. 3c). Using this method, particles and cells could be guided up and over a 20 μm PDMS wall into the neighboring micro-well (lower panel, Fig. 3c) along curved parabolic trajectories.

(ii) Microfluidic sorting using optical control

In addition to transport, precise sorting of microscopic objects in microfluidic environments has been a challenging endeavour. While dielectrophoretic and magnetic field based approaches were mostly exploited in the past for sorting, there is considerable interest in utilization of the optical forces (both scattering and gradient) exerted by laser beams to separate microscopic particles based on their size and their refractive index. In early incarnations of optical chromatography,[13] particles were separated based on their positions which were determined by the balance of scattering force from a weakly focused laser beam with counter-propagating fluid flow (Fig. 3d). Thus, different components of a mixture of uniformly sized polystyrene, PMMA, and silica beads could be optically separated,[13] based on the interaction force (dependent on refractive index) with the laser beam (Fig. 3d). Recently, fluorescence-activated optical force switching-based[44] sorting has been demonstrated in a microfluidic platform (Fig. 3a). This microfluidic-sorting,[44,54] uses an active optical switch (by rapidly scanning optical tweezers), and is demonstrated to be highly efficient with reduced complexity of the chip and simplified connectivity.

Transport of microscopic objects of different sizes or refractive indices can be modulated by microfluidic flow and they can be sorted based on the varied interactions of optical forces and fluid flow. Passive control of cell routing is also possible *via* optical tweezers which may not require further sample processing, such as staining (for fluorescence-identification). For example, since transportation speed of microscopic objects subjected to asymmetric optical tweezers[49] (Fig. 3b) is dependent on the sizes and refractive indices of particles, pure optical separation of microscopic objects in a passive manner is possible. Indeed, aberrated (astigmatic and coma) line tweezers-based transport,

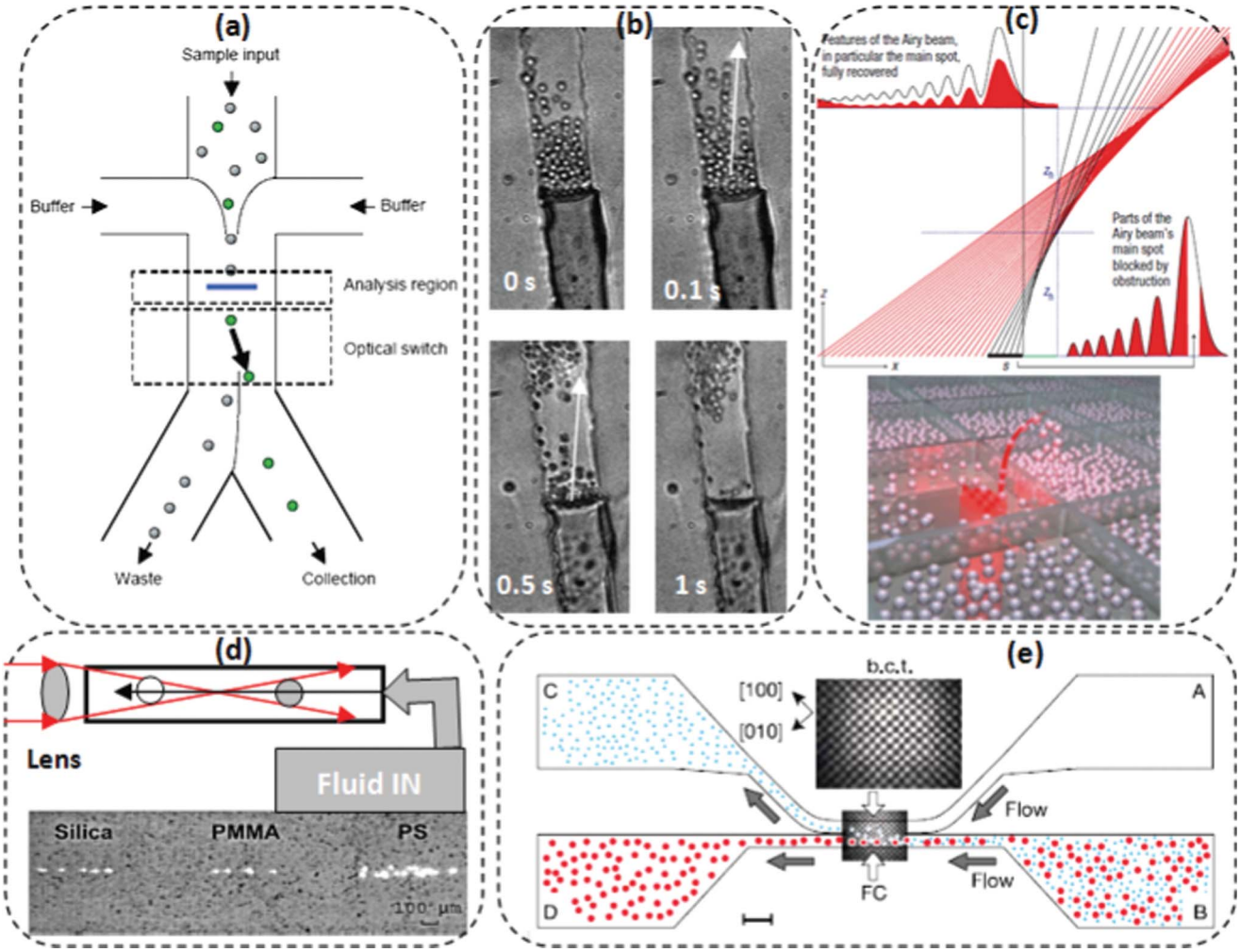

Fig. 3 Optical transport and sorting. (a) Principle of microfluidic sorting with an active optical switch[44] actuated by scanning optical tweezers. (b) Time-lapse images of transportation of microspheres inside a microfluidic channel using asymmetric passive line tweezers[49] (marked by the arrow). Normal incidence leads to symmetric line tweezers and an asymmetric intensity profile (potential well) is generated for tilted incidence. (c) An intuitive representation[50] of a self-healing Airy beam. Rays colored black are blocked by the obstruction (thick black bar, *s*), leading to the red-shaded intensity profile (bottom-right), which is healed (as shown in the upper left corner) after a certain axial distance. Also shown below is the picturesque representation of transportation[10] of objects over the wall into the neighboring micro-well. (d) Optical chromatography principle and separation of uniformly sized PS, PMMA, and silica beads.[13] (e) Concept of optical fractionation of a mixture of objects in chamber B in a periodic landscape.[51] 3D optical lattice (*e.g.* body-centered tetragonal) introduced into the fractionation chamber (FC). One species is selectively pushed into the upper flow field (chamber C). Lower image of part (c) reproduced from Ref. 10.

along with microfluidic flows or electric field induced forces, have been used[55] to deflect microscopic particles of different physical properties. Higher order aberration, such as pincushion distortion, in optical tweezers has been recently employed[56] for optical isolation of objects based on their size. While large (>10 μm) microscopic objects were trapped in the center of the pincushion profile, smaller microscopic objects could be routed along the curvilinear trajectories of the pincushion profile in the distorted optical tweezers. This enabled efficient isolation of cells from their surroundings and thus opens up new possibility to control and study interactions of cells (and other microscopic objects) with surrounding objects without requiring the presence or actuation of physical valves.

For high throughput, passive optical fractionation of microscopic objects, periodic landscapes in 2D[57] as well as 3D[51] have been generated either holographically,[57] by interference,[51] or by use of an acousto-optic deflector.[58] When a three-dimensional optical lattice[51] was introduced into the fractionation chamber, one species of objects (from chamber B, Fig. 3e) can be selectively pushed into the upper flow field (chamber C). In this case, since the optical lattice can be reconfigured, dynamic updating of the selection criteria can be made. Further, up to four different sizes of colloidal microparticles have been sorted simultaneously into laterally-separated laminar streams using a 2D potential landscape, generated by an acousto-optic deflector.[58] It may be noted that to increase the purity of the isolated species, the sample can be routed through cascaded separation chambers having increasingly selective conditions. Further, selective species can be attached to plastic beads to improve their isolation efficiency. Such a method has been applied in Bessel beam sorting, where CD2 T-lymphocytes have been isolated from a sample of mononuclear cells.[59] The bead-labeled

cells travel into the central maximum of the Bessel beam and move within the core until they reach the top of the sample chamber where they form a vertical stack. The un-attached cells or smaller particles remain trapped in the rings of the Bessel beam.[59] Multiple Bessel beams can be generated and controlled[60] for parallel optical manipulation and sorting.

Sorting nanoscale objects by optical tweezers has been a challenging task until now, owing to the weaker force on nanoparticles as compared to microscopic objects. However, to overcome this, one can utilize the fact that different materials may respond effectively only to a narrow range of predetermined light frequencies. For example, a laser tuned to resonate[41] with the internal energy levels of semiconductor nanoparticles could pave the way towards size- and shape-selective sorting. Further, optical binding forces may also be useful in the near-future for passive guidance and sorting of nanoscale objects without any external control.[61] Since the optical forces on metallic and semiconductor nanotubes are different, separation of these would also be possible. Indeed, optoelectronic tweezers (Fig. 2d) have been employed to separate semiconducting and metallic nanowires.[35] For example, while a silver nanowire can be transported at speeds up to 125 μm s^{-1}, silicon nanowires experience speeds less than 2 μm s^{-1} for the same conditions[35] owing to the higher polarizability of the silver nanowires. Thus, by scanning the optoelectronic line tweezers with speeds greater than 2 μm s^{-1} silver and silicon nanowires could be separated from each other. Optical fractionation of microscopic objects, based on their size, refractive index and shape in a microfluidic environment is opening up new vistas in colloidal sciences, nanotechnology and biophysical research. However, the true potential of optical fractionation for biomedical analysis in a lab-on-a-chip platform can be achieved by improving the sensitivity of the method to changes in cellular morphology and/or biophysical properties during disease progression.

(iii) Optically-driven rotation for microfluidic actuation

In addition to trapping and transportation, optical tweezers can exert torque on microscopic structures by acting as an optical spanner. This is realized either by spatial structuring of the micro-structure, spatially sculpting the intensity profile of the tweezers beam, or by configuring its phase and polarization.[62] Fig. 4 is a comprehensive representation of various schemes that can be used for rotational actuation in microfluidic environments. Pre-designed micromotors can be fabricated by two-photon polymerization or silicon etching so as to rotate[63] like a windmill by introducing orbital angular momentum to the scattered light in conventional optical tweezers (Fig. 4a). Even engaged cogwheels rotated by a light-driven rotor have been conceived (lower panel of Fig. 4a). Further, asymmetric biological structures such as red blood cells (RBC) in a hypertonic buffer have been shown[64] to rotate in optical tweezers using similar mechanism.

Even symmetric objects (such as spheres) can absorb or scatter a fraction of light from Laguerre–Gaussian (LG) beams carrying orbital angular momentum and thus rotate.[65] The LG beam exhibits a dark spot in the center, and a ring-like intensity profile. The spiraling phase (Fig. 4b) makes the local momentum of the beam mimic the velocity pattern of a vortex fluid.[66]

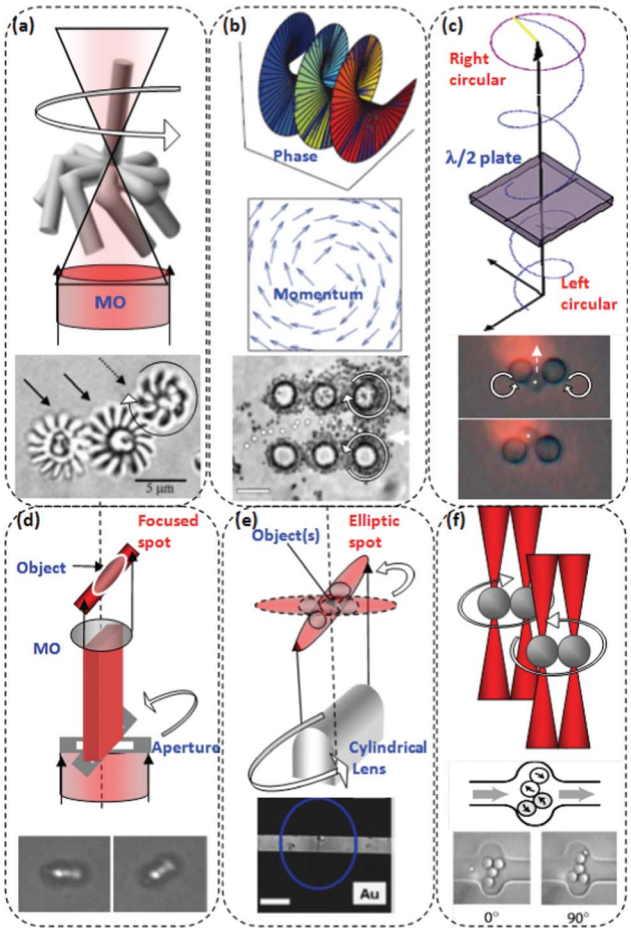

Fig. 4 Optically driven rotation. (a) Transfer of momentum to an asymmetric object. The solid arrows point to the cogwheels rotating on axes fixed to the glass surface. The dashed arrow points to the rotor which is held and rotated by the laser tweezers and the rotating propeller drives the system.[63] (b) LG beam and transfer of orbital angular momentum (AM). The phase of the beam twists around the central dark spot, producing a staircase-like phase wave-front.[66] Composite of 16 time-lapse images in 0.5 s intervals of colloidal spheres in the holographic pump created with holographic optical tweezers made up by LG modes that carry orbital AM and create ring-shaped traps.[8] The trapped silica particles circled the ring centers to create an effective flow. The open circles identify the trajectory of a single sphere as it moves 25 μm to the left in 7 *sec.* (c) Principle of transfer of spin AM and rotation of a birefringent micromotor. Two vaterite particles were made to counter-rotate in dual beam optical tweezers[67] thereby moving a third particle through the space in between them. (d) Rotating aperture based rotation method; sequential frames showing synchronous rotation of a fused assembly of silica spheres.[68] (e) Principle of rotating line tweezers;[69] orientation of CuO nanorod to bridge across Au electrodes.[70] Scale bar = 15 μm. (f) Multiple active tweezers beam-based rotation for optical peristaltic pumping of fluid.[71]

Trapped silica particles can be seen to circle around the ring centers of the multiple LG optical tweezers[8] so as to create an effective flow (lower panel of Fig. 4b).

Rotation of birefringent motors is possible in circularly polarized tweezers carrying spin angular momentum (Fig. 4c). Since transfer of spin angular momentum depends on the laser power, degree of polarization and the thickness and birefringence of the micromotor, control of rotation speed can be easily

achieved.[72] As shown in Fig. 4c, two vaterite particles were made to counter-rotate in dual beam optical tweezers, thereby actuating the fluid (as seen by movement of a tracer particle) through the space in between them.[67] Microfluidic components having form-birefringence can also be rotated by polarized laser tweezers.[73] Efficient micro-circulation of a liquid at its interface with air can be induced by fast rotating beads, driven by either spin or orbital angular momentum transfer, allowing tailored dynamic flow of particles and liquid within the surface. Such an approach may contribute to the improvement of surfaces with respect to friction[74] and hydrodynamic interactions at a vessel wall.[75]

Microscopic objects can also be rotated in a highly controlled manner by rotating an elliptic beam generated either by a rotating aperture[68] (Fig. 4d) or a cylindrical lens[69] (Fig. 4e). These methods are highly suitable for non-spherical objects such as nanorods, which align themselves along the major axis of the elliptic beam profile. The lower panel of Fig. 4e shows the orientation of a CuO nanorod to bridge across Au electrodes using line tweezers generated by orientation of a cylindrical lens.[70] In these cases, transfer of orbital angular momentum arises as a consequence of the change in spatial distribution of the intensity of the linear optical field. Notably, rotation of a cellular assembly and intracellular objects has been achieved using rotating line tweezers.[69] The advancements in optical tweezers technology, such as dynamically-modulated multiple tweezers and rotation, is also enabling complex microfluidic actuations,[71] such as realization of a micro-peristaltic pumps and optically actuated valves. Images in Fig. 4f show the realization of an optically driven peristaltic pump in a microfluidic channel.[71] Here, multiple optical tweezers trapped four particles and each pair of particles is rotated in opposite directions as shown in the upper panel of Fig. 4f. It is important to note here that torque on the microscopic object can be applied along different axes (other than the optical axis) by engineering[76–78] the optical tweezers, thus allowing complete non-contact manipulation.

Besides microfluidic actuation, these miniature rotating devices may find applications as powerful instruments to measure the properties of microscopic systems: for example to determine the torsional rigidity of single particles, biological polymers such as DNA, proteins and to measure microscopic viscosity, *etc.* Rotational actuation of cells[78] can lead to improved tomographic imaging and disease diagnosis in lab-on-a-chip environments. For example, rotation speed of optically-trapped RBC in a hypertonic environment has been shown[64] to be significantly lower (upper panel, Fig. 5a) in the case of malaria-infection. The high-speed self-rotation of the normal RBC in a hypertonic buffer (lower panel, Fig. 5a) arises[64] due to the torque generated on the cell by transfer of linear momentum from the trapping beam.

The laser-driven, RBC micromotor can be seen (lower panel, Fig. 5a) to induce microfluidic flow, leading to movement of tracer object (another RBC). For a given osmolarity (1250 mOsm kg^{-1}), rotational speed increases with an increase in trapping-beam power. The malaria parasite-infected cells (as confirmed by fluorescence staining) were not observed to rotate, even at the highest trap power used in the experiment. The other non-fluorescent RBCs in the blood sample having cells showing acridine orange fluorescence were observed to rotate, but with

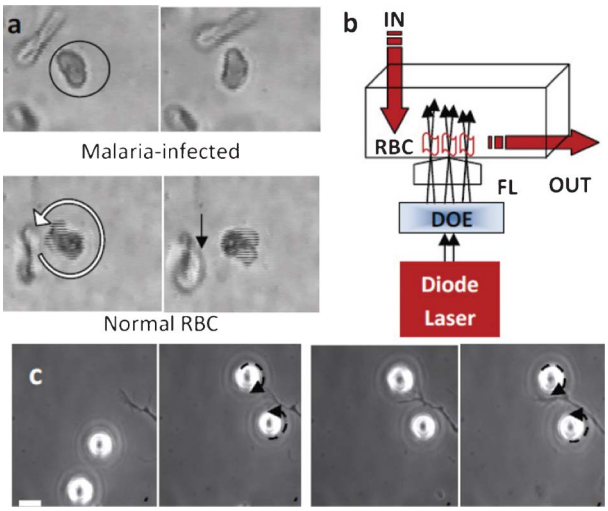

Fig. 5 (a) Time-lapse images of rotation of malaria-infected and normal RBCs in optical tweezers. Direction of rotation is marked by curved-arrow and direction of flow by straight arrow. (b) Schematic of the optofluidic chip for high throughput malaria diagnosis. DOE: Diffractive optical element, FL: focusing lens. (c) Time-lapse images of optofluidic manipulation of axonal guidance.[82] The optofluidic flow was generated by trapping and rotating two vaterite particles in opposite directions at 1 Hz.

lower speeds than normal RBCs. These observations are consistent with the fact that the rigidity of malaria-infected cell membranes is an order of magnitude larger than that for normal cells.[79] Further, it is known that mature parasites release *exo*-antigens, which increase the rigidity of the uninfected RBCs in the sample.[80,81] The large difference in rotational speed at a given trap beam power can be exploited for detection of malaria infected cells.

To further extend this method, diode laser based optical tweezers can be combined with microfluidic chips so as to realize a compact and inexpensive analysis device. Fig. 5b shows a schematic of an optofluidic chip which consists of multiple optical tweezers (generated using diffractive optical element) so as to achieve high throughput screening. Recently, microfluidic flow generated by the optical tweezers-assisted rotation of birefringent particles[72] has also enabled guidance of axons.[82] Fig. 5c shows time-lapse images of axonal growth cone guidance through two rotating vaterite particles. Such optically-controlled fluid manipulation allowed precise spatio-temporal applications of fluid flow near the growth cone, thus removing the need for on-chip plumbing.

C. Microfluidic characterization using optical tweezers

(i) Mapping properties of microfluidic environments

In addition to actuating microscopic objects, optical tweezers have been extensively explored as a sensor for the interaction between soft matter, including colloids. Knowledge of the dynamics and of the forces acting between colloidal particles is mandatory for understanding the stability of nanoparticle suspensions,[83] electrostatics[84] being one important class on such forces. Further, differences in the micro- and macro-rheological properties of complex fluids can be quantified by optical

tweezers.[85] Colloids in viscoeleastic (in contrast to only viscous) solutions may be of technical importance for nano/micro-machines and single biomolecular function.

While optical tweezers-based actuation allows control of fluid flow in microfluidic channels, it can also probe microviscosity and other key properties of the microfluidic environment in a non-contact manner. For example, optical tweezers has been used[86] as a sensor for direct mapping of shear stress acting on microspheres at arbitrary positions in microfluidic systems of different internal geometries (straight as well as curved). The flow and mixing of fluids through microfluidic circuitry is highly dependent on the viscosity of the fluids. Further, on the microscopic scale, viscosity plays a major role in the dynamics of physical, chemical, and biological systems. For example, the dynamics of a protein molecule and its interaction with other molecules is affected by the viscosity of the medium around it.

Scanning optical tweezers have been employed[29] for spatial mapping of microscopic viscosity in a minimally invasive manner which is not only fast but also does not require fluorescent probes. In this case, the trapped microsphere was actuated back and forth by the scanning laser tweezers and light scattered from the focal point of the tweezers was confocally detected. The resulting particle motion is periodic, with a frequency equal to the driving frequency of the laser tweezers and a phase lag due to the hydrodynamic drag. By measuring this phase lag, the characteristic time constant of the motion (proportional to the medium's viscosity) was determined.[29] An image of the viscosity distribution around a biopolymer (pullulan)-producing cell of *Aureobasidium pullulans* is shown as an example[29] (Fig. 6a). In this case, the bead (marked by an arrow) was moved in steps of 0.53 μm, and the frequency of the optical tweezers (19 mW) oscillation was 300 Hz. The sharp gradient of viscosity in the 16 × 16 map (arrow marked rectangle in the bright-field image) can be clearly seen around the cell. Such measurements of viscosity in and around the cell can provide valuable input on the diffusion and transport processes of macromolecules involved in most of the other cellular functions, such as protein synthesis, signaling and migration. It may be noted that the optical tweezers-based rotation has also been used[87,88] for measuring microscopic viscosity.

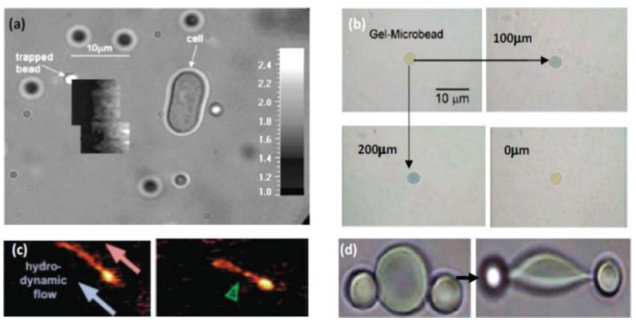

Fig. 6 Characterization by optical tweezers. (a) Viscosity map obtained by scanning optical tweezers-based viscosity microscope,[29] the vertical bar represents viscosity (scale) values relative to the viscosity of water. (b) Spatiotemporal mapping of pH of solvent by a gel-microbead trapped[30] in scanning optical tweezers. (c) Stretching of a single DNA molecule, followed by restriction analysis.[89] (d) Stretching and measurement of elasticity of single cell by dual optical tweezers.[90] Part (b) reproduced from Ref. 30.

In addition to viscosity, pH and temperature play very important roles in the synthesis of new materials by chemical and physical reactions or by biological processes. Therefore, there is a growing demand for measurement of the local pH and temperature distribution in and around biological cells and in microfluidic chips.[91] Conventional pH measurement requires a probe to be deployed in an open space; the motion of which creates disturbances in the environment. Most importantly, the measurement area of the sensor is limited by the sensor size and the fact that measurements made in a finite closed space (*e.g.* in microfluidic chips) are not possible. Optical tweezers provide a unique, controlled way of sensing the pH of a solution with high spatial and temporal sensitivity by positioning a microparticle modified with a pH-sensitive fluorescent dye.[57] In order to avoid problems of bleaching in long-time measurements, hydrophilic gel microbeads, impregnated with the pH indicator bromothymol blue (BTB), have also been used[30] (Fig. 6b). Since the pH value is measured from the optical (fluorescence or absorption) image of the probe particle, wiring of the sensor is avoided, allowing 3D local pH measurements by non-contact manipulation. This method of optical tweezers–assisted probing can be extended to temperature mapping by use of microscopic probes carrying temperature-sensitive dye.[91] However, care must be taken in order to avoid heating due to the optical trapping beam itself.[92]

(ii) Characterization of samples in microfluidic environments

Single beam, near infrared (NIR) optical tweezers[7] provide unprecedented precision in investigating and manipulating microscopic objects; especially the living cells[93] and molecules inside sterile and closed environments. This allows long-term force and spectroscopic analysis of motile cells and molecules being immobilized by the tweezers without perturbing their natural environment. Another advantage of optical tweezers-based analysis is that the manipulation beam can also be simultaneously used for excitation of fluorescence[94,95] and Raman[96] spectroscopy of motile objects. As well as local measurement of the interaction of molecules (such as RNA-polymerase[97] with DNA or kinesin/myosin[98] with microtubules), the mechanical property of the whole macromolecules (such as DNA or microtubules) can be measured[60] by optical tweezers. For measurement of biophysical properties of a single DNA molecule, either both or one end of the molecule can be coupled to microscopic beads, which can then be trapped and stretched by optical tweezers. Thus, the elasticity (from elongation *vs.* applied force) of DNA molecules can be measured under different chemical conditions. Fig. 6c (left panel) shows trapping of one end of a DNA molecule that was stretched by hydrodynamic flow.[89] The right panel of Fig. 6c shows enzymatic (restriction endonuclease EcoR I) digestion (at the arrow marked position) of a single hydrodynamically stretched lambda-DNA molecule (all five expected restriction sites have been observed[89]). Since restriction sites are dependent on the DNA sequence, such methods can be highly useful for accurate forensic analysis of small samples in lab-on-a-chip devices, whereas other techniques, such as PCR, are limited.

Similar to single molecules, the mechanical properties of single cells can be quantified by optical tweezers with force extending into the hundreds of pN. The mechanics of vesicles and cells[99] are crucial for a wide variety of life processes, from cell transport in microcapillary blood vessels to cancerogenesis, as well as ageing, when blood vessels become stiff. Conventionally, beads (high refractive index) are attached to act as handles on cells providing avenues to apply larger force by the optical tweezers. This method has been recently used[100] in a microfluidic system to locally apply tensile and compressive force on selected cells for study of mechanotransduction and focal adhesion. Fig. 6d shows stretching of a single red blood cell by dual optical tweezers holding two beads coupled to two diametrically opposite points.[90] This method has been used to probe the change in elasticity of the cell membrane during progression of disease, especially in various stages of malaria where the cytoskeleton stiffens due to certain proteins released by the parasite. Other diseases studied with this method include cancer,[90] and thalassemia[101] *etc.* However, the additional step of bead attachment and active movement of optical tweezers can be avoided by combination of fluid flow and static optical tweezers. Optofluidic stretching has been successful[102] in evaluating the viscoelastic properties of fresh and stored RBC. The viscous drag force required for deformation > 0.1 μm of a stored RBC was found to be $\sim$10 pN as compared to $\sim$4 pN required for fresh RBC. This shows decreased deformability of aged cells as compared to fresh cells. From the slope of the linear fit (1/2 πμ) to the variation of diameter of the RBC along axis of compression as a function of the viscous force, surface shear modulus of elasticity (μ) can be estimated. Optofluidic stretching can be also employed to measure adhesion force between two adhered RBCs. With the use of multiple optical tweezers in conjunction with microfluidic flow, the throughput of the stretching analysis can be increased so as to have diagnostic and drug-screening applications.

While multiple fluidic tasks can be achieved on a microfluidic-chip, most optical components such as the laser, beam deflection and focusing devices, required to generate optofluidic actuation and characterization have been kept out of the chip. Although this open-optics environment allows better reconfigurability of the laser beams, it has several disadvantages (such as complexity, bulkiness and tendency for misalignment) associated with it while pursuing specific applications. Therefore, in order to make optical force-based optofluidic devices portable and sensitive for various point-of-care diagnostics applications, integration of optical elements[103] into microfluidic devices is essential.

D. Fiber optical manipulation

(i) Trapping and transport using fiber-optic beams

Due to easy integration with microfluidic devices, fiber optical trapping is finding increasing use for actuation as well as analysis of microscopic objects. Further, the low working distance of high NA objectives, like those employed in conventional optical tweezers, severely limits the depth at which objects can be manipulated and analyzed. Via fiber-optic delivery of laser beams, manipulation of microscopic objects can be easily carried out in lab-on-a-chip devices, in contrast to bulky and expensive free-space optical traps. Counter-propagating beams emanating from two single-mode cleaved optical fibers have been used for trapping of microscopic particles[104] and cells.[105] In this approach, scattering forces from two opposing directions leads to axial trapping at the equilibrium point while gradient forces arising due to Gaussian nature of the two beams leads to transverse trapping in the optical axis. In contrast to microscope objective based conventional optical tweezers, the counter-propagating dual fiber-optic trap configuration provides large trapping volume with low power density, which is ideal for cellular studies due to reduction in possible sample damage. Such counter-propagating dual fiber-optic traps have also enabled the formation and manipulation of self-organized assemblies of colloidal particles by optical binding.[106]

For increasing the trapping efficiency of the fiber optic trap, the tip of the optical fiber has been modified[107] into hemi-spherical lenses (Fig. 7a). However, the single-beam fiber with a spherical lens tip could only trap objects in two-dimensions.[108] This can be attributed to the fact that the spot size is large, owing to the finite mode field diameter of the fiber, and also the fact that the spherical microlens is not free from aberrations. The aberration and large Rayleigh range (also large spot size) leads to a smaller restoring force in the axial direction as compared to the opposing scattering forces. Therefore, in the dual-beam fiber traps, for stable trapping of microscopic objects in 3D, the counter-propagating laser beams from the two fibers, with cleaved[104] or lens[107] ends, have to be perfectly aligned. Even use of a tapered, hollow tip,[109] or small tip-cone angle-axicon fiber tip,[110] for trapping required an additional counter-balancing force of non-optical origin. Though the small tip-cone angle axicon-fiber has been used for organizing linear chains of particles by optical binding,[111] the Bessel beam generated by small tip-cone angle axicon-fibers leads to interesting scattering force-induced transportation behavior[112] as compared to diverging Gaussian beam from cleaved fiber. However, engineering large tip cone angles has led to reduced scattering forces as compared to the axial gradient force in the case of micro-axicon tipped fibers. Various axicon tips can be formed by chemical or focused ion beam etching. In the selective chemical etching method,[113] the tip formation takes place at the interface of the etching hydrofluoric acid (HF) and the protecting organic layer

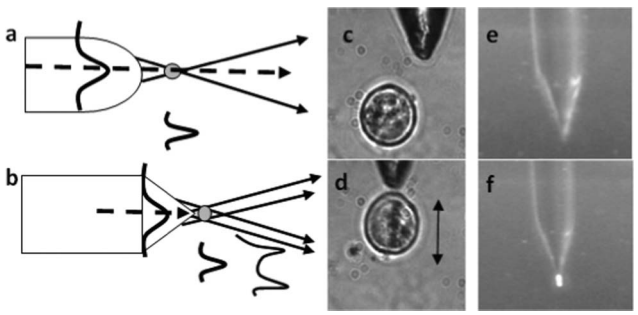

Fig. 7 Schematic of the beam propagation through (a) a micro-lens, and (b) a micro-axicon built on tip of the fiber. (c–d) Fiber-optical trapping[15] of a neuroblastoma cell (c: before and d: after trapping). (e) The axicon fiber tip inside a cuvette containing 3 μm fluorescent polystyrene particles, visualized by a side-viewing objective using bright field. (f) Two-photon excited fluorescence[115] of the trapped particle along with bright-field.

(*e.g.* toluene). The cone angle of the fiber tip in this process is determined by the contact angle of HF with the fiber. The etching process is self-terminating and the cone angle is influenced by the liquid used as top protection layer. For fabrication of a larger tip-cone angle, a two-step etching technique[114] has been used.

3D trapping using a fiber axicon microlens is possible[15] due to nearly diffraction-limited focusing[116] and the characteristic Bessel-Gauss beam profile (Fig. 7b) which emerges from the (large tip cone-angle) micro-axicon tip fiber. Single fiber 3D optical trapping has been used for trapping (Fig. 7c–d), as well as the stretching of cells (Fig. 7d). Further, by using an ultrafast laser beam for trapping, two-photon excitation (Fig. 7 e–f) of the trapped particle can be achieved using the trapping beam itself.[115] Thus, the single fiber manipulation beam can be easily integrated with lab-on-a-chip devices for trapping, transport and biophysical (biochemical) analysis. Further, multiple fibers can be arranged in the microfluidic platform to increase throughput and to sort microscopic objects based on their size and/or refractive index differences. Indeed, fiber-optic microfluidic sorting of microscopic particles has been demonstrated[112] using a static orthogonal configuration of two fibers; one having a micro-axicon on the tip and the other fiber being cleaved. Since the micro-axicon (small tip-cone angle) fiber produces a focused Bessel-like beam, which has a central dark region (Fig. 7b), after a characteristic propagation distance, a very small fraction of the power travels with rays nearly parallel to the optical axis. Therefore, with increasing separation, almost no rays interact with the particles from the fiber tip, and thus, the scattering force is substantially reduced. Therefore, the speed of the particle(s) at different distances from the micro-axicon tip depend much more critically on the particle size in contrast to the beam generated by a cleaved fiber. These differences in the speed of transportation of microscopic objects were exploited to sort the microscopic objects based upon their size in a static manner by simultaneous use of the micro-axicon-tipped fiber and the cleaved fiber in an orthogonal geometry. Thus an optofluidic device with more complex beam profiles, fiber configurations and channels can be developed for the interrogation and efficient sorting of particles. The throughput of the whole process can be improved by the integration of an array of fiber tips into the microfluidic platform. Parallel manipulation of microscopic objects has been shown earlier[117] by a fiber-bundle and lens-based optical tweezers array, in which a digital micro-mirror was used for controlled manipulation of the array.

(ii) Fiber-optic rotation of microscopic objects

The conventional microscope objective based laser spanners (based on transfer of spin or orbital angular momentum) are limited in the depth at which they can actuate microscopic objects in a microfluidic environment. Though depth-limitation can be overcome by the use of fiber-optical microbeams, controlled rotation of fiber-optically trapped objects has been very challenging and is still evolving. Herein, we will describe three fiber-optic rotation methods which have promise for actuation in microfluidic environment.

Käs' group has developed a dual-fiber method[118] in which the trapped microscopic object is rotated by active rotation of one of the fibers around the optic axis. This method uses one non-rotationally symmetric trapping beam, which results from the excitation of higher order modes in a dual-mode optical fiber. Objects such as RBC, having shape anisotropy, follow the rotation of the beam asymmetry (Fig. 8a to c), similar to the microscope-objective based method.[69] However, this method is limited to specific axis of rotation and is logistically complex for continuous rotations. Another interesting fiber-optic rotation technique[120] employs single-tapered fibers to rotate trapped, birefringent objects. In this method, the spin angular momentum of elliptically-polarized light delivered by a polarization-preserving fiber is transferred to a birefringent particle, similar to the optical tweezers-based rotation method.[72] Though it is limited to rotation of birefringent objects and the axis of rotation cannot be controlled, this method can actuate micromotors continuously. Further, it may be noted that in cases of spin angular momentum-based optical rotation[72], speed of rotation can be controlled by varying the degree of elliptic polarization as well as by the control of laser beam power. The third fiber-optic method[119] has been recently developed by us for controlled rotation of microscopic objects. This method utilizes scattering and gradient forces from two transversely-misaligned, counter-propagating fiber-optic beams (Fig. 8d). Similar to a dual beam trap, the gradient forces of the two beams results in a 2D optical trap and the scattering forces push the object along the fiber-optical axis to an equilibrium position between the two fibers. In addition, the scattering forces from the two transversely offset beams generate a torque about the center of the object, causing it to rotate about an axis perpendicular to the fiber-optical axis.

Using the dual fiber transverse-offset method,[119] a planar microstructure (formed by aggregation of seven adhering polystyrene microspheres) has been stably trapped with the plane parallel to the fiber optic axis (Fig. 8 d to f). Not only could the structure be rotated, but it could also be moved while being rotated by changing the relative power of the two fiber-optic beams. The rotation speed of the trapped object can be controlled in a linear manner by adjusting the laser beam power coupled to the fibers. This dual fiber transverse-offset method[119]

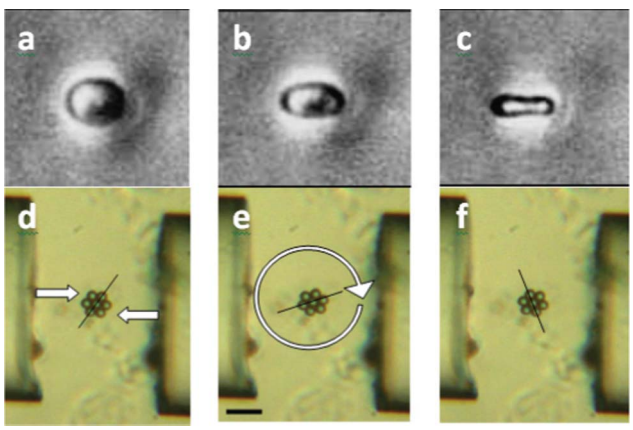

Fig. 8 (a–c) Phase contrast images of the fiber-optical rotation of a red blood cell by active rotation of a fiber emitting dual-mode beam profile.[118] (d–f) Transversely-offset dual fiber based rotation method;[119] time-lapse images of fiber-optic rotation of a micromotor. Straight arrows (d) indicate scattering force from the two fiber optic beams and curved arrow (e) indicates direction of rotation. Scale bar: 20 μm.

does not limit the sample to possess special structural or optical properties in order to be rotated. Since there is no active mechanical movement needed for driving rotation, the fibers can easily be integrated into lab-on-a-chip devices. It is important to note here that torque can be applied along different axes by creating desired offset between the two fiber optic arms, thus allowing complete non-contact manipulation of microscopic objects. With unrestricted rotation axis, tomographic microscopy of objects in microfluidic environments can benefit from fiber-optical rotation. Further, incorporation of multiple optical fibers at different angles will enable complex microfluidic actuation. For micromotors and cogwheels fixed to substrates, a single fiber can drive the micromotor by exerting a scattering force near the edge of the motor. However, for reversing the direction of rotation, a counter-propagating beam would be required. The fiber-optic driven rotation can find potential applications for cellular mechano-transduction[82] by exerting shear stress due to the microfluidic flow near different cellular structures.

(iii) Characterization of fiber-optically manipulated objects

The introduction of fiber-optic trapping[121] allows the possibility of a whole host of studies, such as stable trapping of microscopic objects for spectroscopic characterization,[122,123] and stretching of cells for disease diagnosis[124,125] based on altered biomechanical properties. Apart from miniaturization capability, optical fiber based manipulation can be used in multi-functional modes such as sensing and disease diagnosis in microfluidic environments. Indeed, positional control, along with fluorescence detection of chemically treated beads, have been demonstrated[126] by a multi-fiber geometry in a microfluidic environment.

The dual fiber optical trap (called the optical stretcher[127]) has been used[124,125] to study changes in single cells (Fig. 9a) without requiring the attachment of beads (as in conventional optical tweezers), allowing easy interrogation of cells under microfluidic flow. In this case, counter-intuitively, the scattering force on the surfaces of soft microscopic objects (*e.g.* cells) stretches the surface towards the fiber. Due to divergent beams from the two fibers, the trapping volume is large with lower power density, which offers significant advantages in trapping large objects with reduced photodamage. This method permits the analysis of a large number of individual cells by incorporation of an automated flow chamber. Further, since changes in the shape of the cell (which is acting as a lens) can alter the light coupled from fiber 1 to fiber 2, an all-optical stretching and analysis technique is possible without the requirement of standard imaging and image analysis processes. It may be noted that even single fiber optical tweezers can be used for both stretching[15] and fluorescence excitation[115] (Fig. 7), and thus alignment of two-fibers may be avoided in microfluidic flow-based characterization of cells.

Immobilization of cells by fiber-optic trapping in a microfluidic environment not only enables further (optical) manipulation of the sample, it also allows sufficient time for the recording of fluorescence and Raman spectra (Fig. 9b), especially from otherwise-motile samples. It may be noted that the fiber-optic trapping beam itself can be used as the fluorescence/Raman excitation source, thus the need for additional sources can be

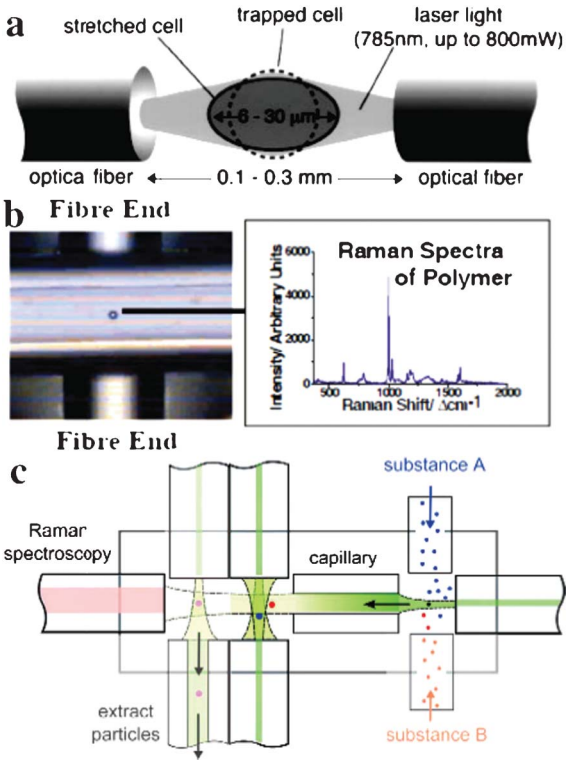

Fig. 9 (a) Schematic of a dual fiber optical stretcher.[128] (b) Dual fiber-optical trap for Raman spectroscopy.[129] (c) Sketch of the all-fiber optical trap and spectroscopy with perpendicular particle injection through a capillary.[130] Part (c) reproduced from Ref. 130.

removed. However, it may require use of collimated or focused beams generated by use of micro-axicon[15,115] or lens on fiber tips. Further, in case of Raman spectroscopic analysis,[123] the ability to trap cell(s) away from the surface by the dual beam fiber optic trap allows avoidance of any spurious signal from the surface and hence reduction in data acquisition time.

Fiber-optical traps and Raman spectroscopy are also becoming powerful tools for optofluidic characterization of airborne microscopic particles. Fiber-optically guided light-beams in a glass capillary have been used[131] to separate single aerosol droplets from an aerosol-flooded injection chamber into a separate sample chamber. Further, integration of conventional optical tweezers with fiber-optical trap-based delivery of aerosol particles (Fig. 9c) allowed on-chip studies of the coagulation of the aerosol particles.[130] With integration of a multi-mode fiber for collection of the Raman scattered trapping light, an all-fiber all-optical single-aerosol particle lab-on-a-chip device has recently been demonstrated (Fig. 9c). The ability to selectively coalesce airborne droplets of different compositions into a controlled environment and chemically analyze them by Raman spectroscopy opens up new vistas for airborne droplet research.

E. Looking forward

We have reviewed key principles of optical manipulation, used to perform a myriad of tasks such as the immobilization, transportation, sorting and rotation of microscopic objects in microfluidic environments, with examples on how such actuation can even be used to probe the micro-environment. Further, we

have presented physical and chemical characterizations, which can be achieved by force and other spectroscopic measurements on optically-manipulated objects. Laser-driven rotation has been shown to control fluid flow in a flexible manner, which is believed to replace the need for on-chip plumbing. The fact that in optical-binding, microscopic particles are coupled to each other, extended microfluidic actuation can be achieved since the optical actuation of one particle enables the movement of other, optically bound objects. Novel methods based on resonant optical tweezers and spectroscopy, which will allow simultaneous trapping and sensitive characterization of microscopic objects, are evolving. Such advancements in optical tweezers technology will expedite the integration of optical purification, construction, characterization, and manipulation of objects at the micro and nanoscopic level.

The challenges encountered by optical tweezers include the depth at which the objects can be manipulated and the throughput that can be achieved. While the use of fiber-based optical tweezers[15,110] can overcome the depth limitation of high NA microscope objectives (utilized in traditional optical tweezers), use of optoelectronic tweezers[35] can significantly enhance the throughput. Advantages of fiber optic manipulation over conventional optical tweezers can be exploited for easy integration with lab-on-a-chip microfluidic platforms. Fig. 10 shows a schematic of a multifunctional fiber optic probe for trapping, transport, two-photon excitation and force measurement (by beam 1); cellular stretching (by beam 2); and generation of localized fluid flow (by beam 3). By multiplexing different light sources, imaging and spectroscopic analysis of the microscopic objects can be achieved with high throughput, especially with novel beams and spatially-sculpted light.

Acknowledgements

The author would like to thank Prof. K. O. Greulich (FLI-Leibnitz Institute, Germany), Dr Ling Gu and Bryan Black (Biophysics Lab, UT Arlington) for their help in preparation of the manuscript. Also thanks to our collaborators for experiments and Stephen Durke for the fiber-optic artwork. Apologies to all authors whose work could not be cited due to space limitations.

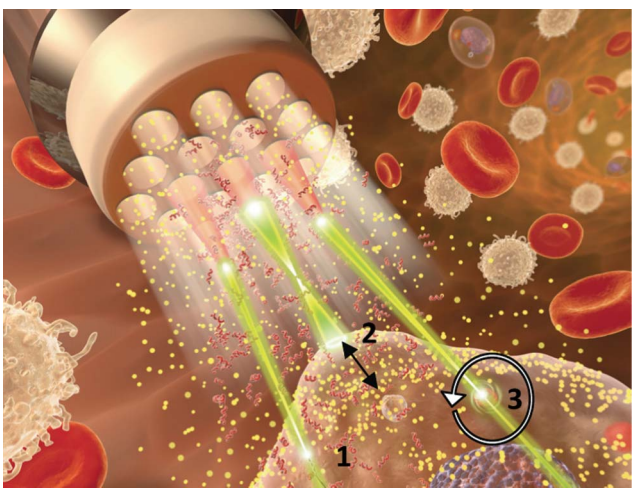

Fig. 10 Schematic of a multifunctional fiber optical probe for (i) trapping, transport and delivery of objects, (ii) force measurement, (iii) two-photon excitation, (iv) cell stretching, and (v) generation of localized fluid flow.

References

1 A. Ashkin and J. M. Dziedzic, *Appl. Phys. Lett.*, 1971, **19**, 283.
2 V. Garces-Chavez, D. Roskey, M. D. Summers, H. Melville, D. McGloin, E. M. Wright and K. Dholakia, *Appl. Phys. Lett.*, 2004, **85**, 4001–4003.
3 A. Ashkin and J. M. Dziedzic, *Science*, 1975, **187**, 1073–1075.
4 G. A. Swartzlander, T. J. Peterson, A. B. Artusio-Glimpse and A. D. Raisanen, *Nat. Photonics*, 2011, **5**, 48–51.
5 S. M. Block, *Nature*, 1992, **360**, 493–495.
6 A. Ashkin, J. M. Dziedzic, J. E. Bjorkholm and S. Chu, *Opt. Lett.*, 1986, **11**, 288–290.
7 A. Ashkin, J. M. Dziedzic and T. Yamane, *Nature*, 1987, **330**, 769–771.
8 K. Ladavac and D. Grier, *Opt. Express*, 2004, **12**, 1144–1149.
9 D. McGloin and K. Dholakia, *Contemp. Phys.*, 2005, **46**, 15–28.
10 J. Baumgartl, G. M. Hannappel, D. J. Stevenson, D. Day, M. Gu and K. Dholakia, *Lab Chip*, 2009, **9**, 1334–1336.
11 K. Svoboda and S. M. Block, *Opt. Lett.*, 1994, **19**, 930–932.
12 L. Paterson, M. P. MacDonald, J. Arlt, W. Sibbett, P. E. Bryant and K. Dholakia, *Science*, 2001, **292**, 912–914.
13 S. J. Hart and A. V. Terray, *Appl. Phys. Lett.*, 2003, **83**, 5316–5318.
14 M. W. Berns and K. O. Greulich, *Laser Manipulation of Cells and Tissues, Academic Press*, 2007.
15 S. K. Mohanty, K. S. Mohanty and M. W. Berns, *J. Biomed. Opt.*, 2008, **13**, 054049.
16 J. Enger, M. Goksor, K. Ramser, P. Hagberg and D. Hanstorp, *Lab Chip*, 2004, **4**, 196–200.
17 P. Korda, G. C. Spalding, E. R. Dufresne and D. G. Grier, *Rev. Sci. Instrum.*, 2002, **73**, 1956–1957.
18 M. Werner, F. Merenda, J. Piguet, R. P. Salathe and H. Vogel, *Lab Chip*, 2011, **11**, 2432–2439.
19 Y. Roichman and D. Grier, *Opt. Express*, 2005, **13**, 5434–5439.
20 P. J. Rodrigo, L. Kelemen, D. Palima, C. A. Alonzo, P. Ormos and J. Glückstad, *Opt. Express*, 2009, **17**, 6578–6583.
21 M. M. Burns, J. M. Fournier and J. A. Golovchenko, *Phys. Rev. Lett.*, 1989, **63**, 1233–1236.
22 S. K. Mohanty, J. T. Andrews and P. K. Gupta, *Opt. Express*, 2004, **12**, 2746–2753.
23 T. M. Grzegorczyk, B. A. Kemp and J. A. Kong, *Phys Rev Lett*, **2006**, 96.
24 D. L. Andrews and J. Rodriguez, *Opt. Lett.*, 2008, **33**, 1830–1832.
25 M. M. Burns, J. M. Fournier and J. A. Golovchenko, *Science*, 1990, **249**, 749–754.
26 T. Cizmar, L. C. D. Romero, K. Dholakia and D. L. Andrews, *J Phys B-at Mol Opt*, 2010, 43.
27 N. K. Metzger, R. F. Marchington, M. Mazilu, R. L. Smith, K. Dholakia and E. M. Wright, *Phys Rev Lett*, 2007, 98.
28 A. Yao, M. Tassieri, M. Padgett and J. Cooper, *Lab Chip*, 2009, **9**, 2568–2575.
29 B. A. Nemet, Y. Shabtai and M. Cronin-Golomb, *Opt. Lett.*, 2002, **27**, 264–266.
30 H. Maruyama, F. Arai and T. Fukuda, *Lab Chip*, 2008, **8**, 346–351.
31 Z. Li, B. Anvari, M. Takashima, P. Brecht, J. H. Torres and W. E. Brownell, *Biophys. J.*, 2002, **82**, 1386–1395.
32 S. Kuo and M. Sheetz, *Science*, 1993, **260**, 232–234.
33 C. Bustamante, S. B. Smith, J. Liphardt and D. Smith, *Curr. Opin. Struct. Biol.*, 2000, **10**, 279–285.
34 J. R. Moffitt, Y. R. Chemla, S. B. Smith and C. Bustamante, *Annu. Rev. Biochem.*, 2008, **77**, 205–228.
35 A. Jamshidi, P. J. Pauzauskie, P. J. Schuck, A. T. Ohta, P.-Y. Chiou, J. Chou, P. Yang and M. C. Wu, *Nat. Photonics*, 2008, **2**, 86–89.
36 K. C. Neuman and S. M. Block, *Rev. Sci. Instrum.*, 2004, **75**, 2787–2809.
37 K. T. Gahagan and G. A. Swartzlander, *J. Opt. Soc. Am. B*, 1998, **15**, 524–534.
38 R. Agarwal, K. Ladavac, Y. Roichman, G. Yu, C. Lieber and D. Grier, *Opt. Express*, 2005, **13**, 8906–8912.
39 N. Calander and M. Willander, *Phys. Rev. Lett.*, 2002, **89**, 143603.

40 S. K. Mohanty, K. D. Rao and P. K. Gupta, *J. Nanophotonics*, 2008, **2**, 023509.
41 T. Iida and H. Ishihara, *Phys. Rev. Lett.*, 2003, **90**, 057403.
42 M. Gu, S. Kuriakose and X. Gan, *Opt. Express*, 2007, **15**, 1369–1375.
43 A. Ehrlicher, T. Betz, B. Stuhrmann, D. Koch, V. Milner, M. G. Raizen and J. Käs, *Proc. Natl. Acad. Sci. U. S. A.*, 2002, **99**, 16024–16028.
44 M. M. Wang, E. Tu, D. E. Raymond, J. M. Yang, H. Zhang, N. Hagen, B. Dees, E. M. Mercer, A. H. Forster, I. Kariv, P. J. Marchand and W. F. Butler, *Nat. Biotechnol.*, 2005, **23**, 83–87.
45 P. Domachuk, M. Cronin-Golomb, B. Eggleton, S. Mutzenich, G. Rosengarten and A. Mitchell, *Opt. Express*, 2005, **13**, 7265–7275.
46 T. N. Buican, M. J. Smyth, H. A. Crissman, G. C. Salzman, C. C. Stewart and J. C. Martin, *Appl. Opt.*, 1987, **26**, 5311–5316.
47 J. Arlt, V. Garces-Chavez, W. Sibbett and K. Dholakia, *Opt. Commun.*, 2001, **197**, 239–245.
48 J. Arlt and K. Dholakia, *Opt. Commun.*, 2000, **177**, 297–301.
49 S. K. Mohanty and P. K. Gupta, *Appl. Phys. B: Lasers Opt.*, 2005, **81**, 159–162.
50 J. Baumgartl, M. Mazilu and K. Dholakia, *Nat. Photonics*, 2008, **2**, 675–678.
51 M. P. MacDonald, G. C. Spalding and K. Dholakia, *Nature*, 2003, **426**, 421–424.
52 M. Khan, A. K. Sood, S. K. Mohanty, P. K. Gupta, G. V. Arabale, K. Vijaymohanan and C. N. R. Rao, *Opt. Express*, 2006, **14**, 424–429.
53 S. K. Mohanty, M. Sharma, M. M. Panicker and P. K. Gupta, *Opt. Lett.*, 2005, **30**, 2596–2598.
54 X. Wang, S. Chen, M. Kong, Z. Wang, K. D. Costa, R. A. Li and D. Sun, *Lab Chip*, 2011, **11**, 3656–3662.
55 F. C. Cheong, C. H. Sow, A. T. S. Wee, P. Shao, A. A. Bettiol, J. A. van Kan and F. Watt, *Appl. Phys. B: Lasers Opt.*, 2006, **83**, 121–125.
56 S. Shivalingaiah and S. K. Mohanty, *Proc. SPIE–Int. Soc. Opt. Eng.*, 2011, **7902**, 790224–790228.
57 P. T. Korda, M. B. Taylor and D. G. Grier, *Phys. Rev. Lett.*, 2002, **89**, 128301.
58 G. Milne, D. Rhodes, M. MacDonald and K. Dholakia, *Opt. Lett.*, 2007, **32**, 1144–1146.
59 G. Milne, K. Dholakia, D. McGloin, K. Volke-Sepulveda and P. Zemánek, *Opt. Express*, 2007, **15**, 13972–13987.
60 T. Cizmar, V. Kollarova, X. Tsampoula, F. Gunn-Moore, Z. Bouchal and K. Dholakia, *Optical Trapping and Optical Micromanipulation V*, **2008**, 7038.
61 T. M. Grzegorczyk, B. A. Kemp and J. A. Kong, *Opt. Lett.*, 2006, **31**, 3378–3380.
62 S. K. Mohanty, K. D. Rao and P. K. Gupta, *Appl. Phys. B: Lasers Opt.*, 2005, **80**, 631–634.
63 P. Galajda and P. Ormos, *Appl. Phys. Lett.*, 2001, **78**, 249–251.
64 S. K. Mohanty, A. Uppal and P. K. Gupta, *Biotechnol. Lett.*, 2004, **26**, 971–974.
65 H. He, M. E. J. Friese, N. R. Heckenberg and H. Rubinsztein-Dunlop, *Phys. Rev. Lett.*, 1995, **75**, 826–829.
66 G. Molina-Terriza, J. P. Torres and L. Torner, *Nat. Phys.*, 2007, **3**, 305–310.
67 S. Parkin, G. Knoner, W. Singer, T. A. Nieminen, N. R. Heckenberg and H. Rubinsztein-Dunlop, *Methods Cell Biol.*, 2007, **82**, 525–561.
68 A. T. O'Neil and M. J. Padgett, *Opt. Lett.*, 2002, **27**, 743–745.
69 R. Dasgupta, S. K. Mohanty and P. K. Gupta, *Biotechnol. Lett.*, 2003, **25**, 1625–1628.
70 Y. Ting, C. Fook-Chiong and S. Chorng-Haur, *Nanotechnology*, 2004, **15**, 1732.
71 A. Terray, J. Oakey and D. W. M. Marr, *Science*, 2002, **296**, 1841–1844.
72 M. E. J. Friese, T. A. Nieminen, N. R. Heckenberg and H. Rubinsztein-Dunlop, *Nature*, 1998, **394**, 348–350.
73 S. L. Neale, M. P. MacDonald, K. Dholakia and T. F. Krauss, *Nat. Mater.*, 2005, **4**, 530–533.
74 A. Jesacher, S. Fürhapter, C. Maurer, S. Bernet and M. Ritsch-Marte, *Opt. Express*, 2006, **14**, 6342–6352.
75 R. Di Leonardo, J. Leach, H. Mushfique, J. M. Cooper, G. Ruocco and M. J. Padgett, *Phys. Rev. Lett.*, 2006, **96**, 134502.
76 S. K. Mohanty, R. Dasgupta and P. K. Gupta, *Appl. Phys. B: Lasers Opt.*, 2005, **81**, 1063–1066.
77 V. Bingelyte, J. Leach, J. Courtial and M. J. Padgett, *Appl. Phys. Lett.*, 2003, **82**, 829–831.
78 S. K. Mohanty and P. K. Gupta, *Rev. Sci. Instrum.*, 2004, **75**, 2320–2322.
79 B. M. Cooke, N. Mohandas and R. L. Coppel, *Semin. Hematol.*, 2004, **41**, 173–188.
80 F. K. Glenister, R. L. Coppel, A. F. Cowman, N. Mohandas and B. M. Cooke, *Blood*, 2002, **99**, 1060–1063.
81 D. G. Read, G. R. Bushell and C. Kidson, *Parasitology*, 1990, **100**, 185–190.
82 T. Wu, T. A. Nieminen, S. Mohanty, J. Miotke, R. L. Meyer, H. Rubinsztein-Dunlop and M. W. Berns, *Nat. Photonics*, 2012, **6**, 62–67.
83 M. T. Valentine, L. E. Dewalt and H. D. Ou-Yang, *J. Phys.: Condens. Matter*, 1996, **8**, 9477.
84 S. K. Sainis, V. Germain, C. O. Mejean and E. R. Dufresne, *Langmuir*, 2008, **24**, 1160–1164.
85 G. Pesce, A. C. D. Luca, G. Rusciano, P. A. Netti, S. Fusco and A. Sasso, *J. Opt. A: Pure Appl. Opt.*, 2009, **11**, 034016.
86 J. Wu, D. Day and M. Gu, *Opt. Express*, 2010, **18**, 7611–7616.
87 S. J. Parkin, G. Knöner, T. A. Nieminen, N. R. Heckenberg and H. Rubinsztein-Dunlop, *Phys. Rev. E: Stat., Nonlinear, Soft Matter Phys.*, 2007, **76**, 041507.
88 Q. Liu, T. Asavei, T. Lee, H. Rubinsztein-Dunlop, S. He and I. I. Smalyukh, *Opt. Express*, 2011, **19**, 25134–25143.
89 B. Schäfer, H. Gemeinhardt and K. O. Greulich, *Angew. Chem., Int. Ed.*, 2001, **40**, 4663–4666.
90 S. Suresh, J. Spatz, J. P. Mills, A. Micoulet, M. Dao, C. T. Lim, M. Beil and T. Seufferlein, *Acta Biomater.*, 2005, **1**, 15–30.
91 V. K. Natrajan and K. T. Christensen, *Meas Sci Technol*, 2009, 20.
92 S. Ebert, K. Travis, B. Lincoln and J. Guck, *Opt. Express*, 2007, **15**, 15493–15499.
93 E. Eriksson, J. Enger, B. Nordlander, N. Erjavec, K. Ramser, M. Goksor, S. Hohmann, T. Nystrom and D. Hanstorp, *Lab Chip*, 2007, **7**, 71–76.
94 Y. Liu, D. K. Cheng, G. J. Sonek, M. W. Berns, C. F. Chapman and B. J. Tromberg, *Biophys. J.*, 1995, **68**, 2137–2144.
95 B. Agate, C. Brown, W. Sibbett and K. Dholakia, *Opt. Express*, 2004, **12**, 3011–3017.
96 C. M. Creely, G. P. Singh and D. Petrov, *Opt. Commun.*, 2005, **245**, 465–470.
97 J. W. Shaevitz, E. A. Abbondanzieri, R. Landick and S. M. Block, *Nature*, 2003, **426**, 684–687.
98 A. Kunwar, M. Vershinin, J. Xu and S. P. Gross, *Curr. Biol.*, 2008, **18**, 1173–1183.
99 C. Poole and W. Losert, *Methods Mol. Biol.*, 2007, **400**, 389–404.
100 P. Honarmandi, H. Lee, M. J. Lang and R. D. Kamm, *Lab Chip*, 2011, **11**, 684–694.
101 A. C. De Luca, G. Rusciano, R. Ciancia, V. Martinelli, G. Pesce, B. Rotoli, L. Selvaggi and A. Sasso, *Opt. Express*, 2008, **16**, 7943–7957.
102 S. K. Mohanty, A. Uppal and P. K. Gupta, *J. Biophotonics*, 2008, **1**, 522–525.
103 D. Psaltis, S. R. Quake and C. Yang, *Nature*, 2006, **442**, 381–386.
104 A. Constable, J. Kim, J. Mervis, F. Zarinetchi and M. Prentiss, *Opt. Lett.*, 1993, **18**, 1867–1869.
105 J. Guck, R. Ananthakrishnan, H. Mahmood, T. J. Moon, C. C. Cunningham and J. Käs, *Biophys. J.*, 2001, **81**, 767–784.
106 K. Dholakia and P. Zemanek, *Rev Mod Phys*, **2010**, 82.
107 E. R. Lyons and G. J. Sonek, *Appl. Phys. Lett.*, 1995, **66**, 1584–1586.
108 K. Taguchi, K. Atsuta, T. Nakata and M. Ikeda, *Opt. Quantum Electron.*, 2001, **33**, 99–106.
109 R. Taylor and C. Hnatovsky, *Opt. Express*, 2003, **11**, 2775–2782.
110 K. S. Mohanty, C. Liberale, S. K. Mohanty and V. Degiorgio, *Appl. Phys. Lett.*, 2008, **92**, 151113–151113.
111 S. K. Mohanty, K. S. Mohanty and M. W. Berns, *Opt. Lett.*, 2008, **33**, 2155–2157.
112 C. Liberale, S. K. Mohanty, K. S. Mohanty, V. Degiorgio, S. Cabrini, A. Carpentiero, E. Ferrari, D. Cojoc and E. Di Fabrizio, *Proc. SPIE–Int. Soc. Opt. Eng.*, 2006, **6095**, F950–F950.
113 P. Hoffmann, B. Dutoit and R.-P. Salathé, *Ultramicroscopy*, 1995, **61**, 165–170.
114 Y.-H. Chuang, K.-G. Sun, C.-J. Wang, J. Y. Huang and C.-L. Pan, *Rev. Sci. Instrum.*, 1998, **69**, 437–439.
115 Y. N. Mishra, N. Ingle and S. K. Mohanty, *J. Biomed. Opt.*, 2011, **16**, 105003–105008.

116 S.-K. Eah, W. Jhe and Y. Arakawa, *Rev. Sci. Instrum.*, 2003, **74**, 4969–4971.
117 J. M. Tam, I. Biran and D. R. Walt, *Applied Physics Letters*, 2006, 89.
118 M. K. Kreysing, T. Kießling, A. Fritsch, C. Dietrich, J. R. Guck and J. A. Käs, *Opt. Express*, 2008, **16**, 16984–16992.
119 B. J. Black and S. K. Mohanty, *Imaging, Manipulation, and Analysis of Biomolecules, Cells, and Tissues X*, 2012, **8225**, 82250B–82256.
120 K. S. Abedin, C. Kerbage, A. Fernandez-Nieves and D. A. Weitz, *Appl. Phys. Lett.*, 2007, **91**, 091119–091119-091113.
121 A. Constable, J. Kim, J. Mervis, F. Zarinetchi and M. Prentiss, *Opt. Lett.*, 1993, **18**, 1867–1869.
122 C. Liberale, P. Minzioni, F. Bragheri, F. De Angelis, E. Di Fabrizio and I. Cristiani, *Nat. Photonics*, 2007, **1**, 723–727.
123 P. R. T. Jess, V. Garcés-Chávez, D. Smith, M. Mazilu, L. Paterson, A. Riches, C. S. Herrington, W. Sibbett and K. Dholakia, *Opt. Express*, 2006, **14**, 5779–5791.
124 J. Guck, S. Schinkinger, B. Lincoln, F. Wottawah, S. Ebert, M. Romeyke, D. Lenz, H. M. Erickson, R. Ananthakrishnan, D. Mitchell, J. Kas, S. Ulvick and C. Bilby, *Biophys. J.*, 2005, **88**, 3689–3698.
125 B. Lincoln, S. Schinkinger, F. Wottawah, F. Sauer, S. Ebert and J. Guck, *Biophysical Journal*, 2003, **84**, 481a–481a.
126 C. Jensen-McMullin, H. P. Lee and E. R. Lyons, *Opt. Express*, 2005, **13**, 2634–2642.
127 J. Guck, R. Ananthakrishnan, T. J. Moon, C. C. Cunningham and J. Käs, *Phys. Rev. Lett.*, 2000, **84**, 5451–5454.
128 J. Guck, R. Ananthakrishnan, H. Mahmood, T. J. Moon, C. C. Cunningham, R. Hallworth and J. Kas, *Biophysical Journal*, 2001, **81**, 767–784.
129 P. R. T. Jess, V. Garces-Chavez, D. Smith, M. Mazilu, L. Paterson, A. Riches, C. S. Herrington, W. Sibbett and K. Dholakia, *Opt. Express*, 2006, **14**, 5779–5791.
130 M. Horstmann, K. Probst and C. Fallnich, *Lab Chip*, 2012, **12**, 295–301.
131 M. Horstmann, K. Probst and C. Fallnich, *Appl. Phys. B: Lasers Opt.*, 2011, **103**, 35–39.

